

Variations in Shale Pore Types and Networks*

Roger M. Slatt¹ and Neal O'Brien²

Search and Discovery Article #80348 (2013)**

Posted December 23, 2013

*Adapted from oral presentation given at Geoscience Technology Workshop, Revisiting Reservoir Quality Issues in Unconventional and Conventional Resources: Techniques, Technologies and Case Studies, Austin, Texas, November 12-13, 2013.

**AAPG © 2013. Serial rights given by author. For all other rights contact author directly.

¹University of Oklahoma, Norman (rslatt@ou.edu)

²State University of New York, Potsdam

Opening Statement

This article demonstrates the variety of pore types and networks in unconventional resource shales. These pore types may vary with shale lithology. A technique for estimating porosity and pore shapes by SEM is presented, along with results of such measurements on a number of shales.

Selected References

Ambrose, R.J., R.C. Hartman, M. Diaz-Campos, Y. Akkutlu, and C.H. Sondergeld, 2010, New pore-scale considerations for shale gas in place calculations: Society of Petroleum Engineers Unconventional Gas Conference, February 23–25, 2010, Pittsburgh, Pennsylvania, SPE Paper 131772, 17 p.

Bustin, R.M., A. Bustin, D. Ross, G. Chalmers, V. Murthy, C. Laxmi, and X. Cui, 2009, Shale gas opportunities and Challenges: Search and Discovery Article #40382 (2009) Website accessed December 4, 2013.

http://www.searchanddiscovery.com/documents/2009/40382bustin/ndx_bustin.pdf?q=%2BtextStrip%3Ashale+textStrip%3Agas+textStrip%3Aopportunities+%2BauthorStrip%3Abustin

Curtis, M.E., R.J. Ambrose, C.H. Sondergeld, and C.S. Rai, 2010, Structural characterization of gas shales on the micro- and nano-scales: Canadian Unconventional Resources and International Petroleum Conference, Calgary, Alberta, Canada, October 19–21, 2010, SPE Paper 137693, 15 p.

Erdman, N., and N. Drenzek, 2013, Integrated Preparation and imaging techniques for the microstructural and geochemical characterization of shale by scanning electron microscopy, *in* W.K. Camp, E. Diaz, and B. Wawak, eds., *Electron Microscopy of Shale Hydrocarbon Reservoirs*:

AAPG Memoir 102, p. 7-14.

Jarvie, D. M., 2012, Shale resource systems for oil and gas: Part 2—Shale-oil resource systems, *in* J. A. Breyer, ed., Shale reservoirs—Giant resources for the 21st century: AAPG Memoir 97, p. 89–119.

Jarvie, D.M., R.J. Hill, T.E. Ruble, and R.M. Pollastro, 2007, Unconventional shale-gas systems: The Mississippian Barnett Shale of north-central Texas as one model for thermogenic shale-gas assessment: AAPG Bulletin, v. 91, p. 475–499.

Jennings, D.S., and J. Antia, 2013, Petrographic characterization of the Eagle Ford Shale, South Texas: Mineralogy, common constituents, and distribution of nanometer-scale pore types, *in* W.K. Camp, E. Diaz, and B. Wawak, eds., Electron Microscopy of Shale Hydrocarbon reservoirs: AAPG Memoir 102, p. 101-114.

Lemmens, H., and D. Richards, 2013, Multiscale imaging of shale samples in the scanning electron microscope, *in* W.K. Camp, E. Diaz, and B. Wawak, eds., Electron Microscopy of Shale Hydrocarbon Reservoirs: AAPG Memoir 102,

Loucks, R.G., R.M. Reed, S.C. Ruppel, and U. Hammes, 2012, Spectrum of pore types and networks in mudrocks and a descriptive classification for matrix-related mudrock pores: AAPG Bulletin, v. 96, p. 1071–1098.

Loucks, R.G., 2010, Petrographic controls on reservoir quality of the Upper Cretaceous Woodbine Group, East Texas field, *in* T.F. Hentz, ed., Sequence stratigraphy, depositional facies, and reservoir attributes of the Upper Cretaceous Woodbine Group, East Texas field: The University of Texas at Austin, Bureau of Economic Geology Report of Investigations No. 274, p. 83–93.

Loucks, R.G., R.M. Reed, S.C. Ruppel, and U. Hammes, 2010, Preliminary classification of matrix pores in mudrocks: Gulf Coast Association of Geological Societies Transactions, v. 60, p. 435-441.

Loucks, R.G., R.M. Reed, S.C. Ruppel, and D.M. Jarvie, 2009, Morphology, genesis, and distribution of nanometer-scale pores in siliceous mudstones of the Mississippian Barnett Shale: Journal of Sedimentary Research, v. 79, p. 848–861.

Loucks, R.G., and S.C. Ruppel, 2007, Mississippian Barnett Shale: lithofacies and depositional setting of a deep-water shale-gas succession in the Fort Worth Basin, Texas: AAPG Bulletin, v. 91, no. 4, p. 579–601.

Milner, M., R. McLin, and J. Petriello, 2010, Imaging texture and porosity in mudstones and shales: Comparison of secondary and ion-milled backscatter SEM methods: Canadian Unconventional Resources and International Petroleum Conference, Calgary, Alberta, Canada, October 19–21, 2010, SPE Paper 138975, 5 p.

O'Brien, N. R., and R. M. Slatt, 1990, Argillaceous rock atlas: New York, Springer-Verlag, 141 p.

Reed, R.M. and S.C. Ruppel, 2010, Nano- and micro-pores in the Cretaceous Eagle Ford Shale, south Texas, USA: GSA Abstracts with Programs, v. 42/5, p. 636.

Reed, R.M., R.G. Loucks, D. Jarvie, and S.C. Ruppel, 2008, Differences in nanopore development related to thermal maturity in the Mississippian Barnett Shale; preliminary results: GSA Abstracts with Programs, v. 40/6, p. 268.

Reed, R.M., and R.G. Loucks, 2007, Imaging nanoscale pores in the Mississippian Barnett Shale of the northern Fort Worth Basin (abs.): AAPG Annual Convention Abstracts, v. 16, p. 115. Search and Discovery Article #90063 (2007) (<http://www.searchanddiscovery.com/abstracts/html/2007/annual/abstracts/lbReed.htm>) (Website accessed December 5, 2013).

Rine, J.M., E. Smart, W. Dorsey, K. Hooghan, and M. Dixon, 2013, Comparison of porosity distribution within selected North American shale units by SEM examination of argon-ion-milled samples, *in* W.K. Camp, E. Diaz, and B. Wawak, eds., Electron Microscopy of Shale Hydrocarbon reservoirs: AAPG Memoir 102, p. 137-152.

Slatt, R.M., and N.R. O'Brien, 2013, Microfabrics Related to Porosity Development, Sedimentary and Diagenetic Processes, and Composition of Unconventional Resource Shale Reservoirs as Determined by Conventional Scanning Electron Microscopy, *in* W.K. Camp, E. Diaz, and B. Wawak, eds., Electron Microscopy of Shale Hydrocarbon Reservoirs: AAPG Memoir 102, p. 37-44.

Slatt, R.M., N.R. O'Brien, A.A. Miceli Romero, and H. Rodriguez, 2012, Eagle Ford condensed section and its oil and gas storage and flow potential: AAPG Annual Meeting Abstracts, unpaginated.

Slatt, R.M., P.R. Philp, Y. Abousleiman, P. Singh, R. Perez, R. Portas, K.J. Marfurt, S. Madrid-Arroyo, N. O'Brien, E.V. Eslinger, and E.T. Baruch, 2011a, Pore-to-regional-scale, integrated characterization workflow for unconventional gas shales, *in* J. Breyer, ed., Shale reservoirs: Giant resources for the 21st century: AAPG Memoir 97, 24 p.

Slatt, R.M., R. Portas, N. Buckner, Y. Abousleiman, N. O'Brien, M. Trans, R. Sierra, P. Philp, A. Miceli-Romero, R. Davis, and T. Wawrzyniec, 2011b, Outcrop-behind outcrop (quarry), Multi-scale characterization of the Woodford gas shale, Oklahoma: AAPG Search and Discovery Article #80138, 22 p. Web accessed December 12, 2013. http://www.searchanddiscovery.com/documents/2011/80138slatt/ndx_slatt.pdf

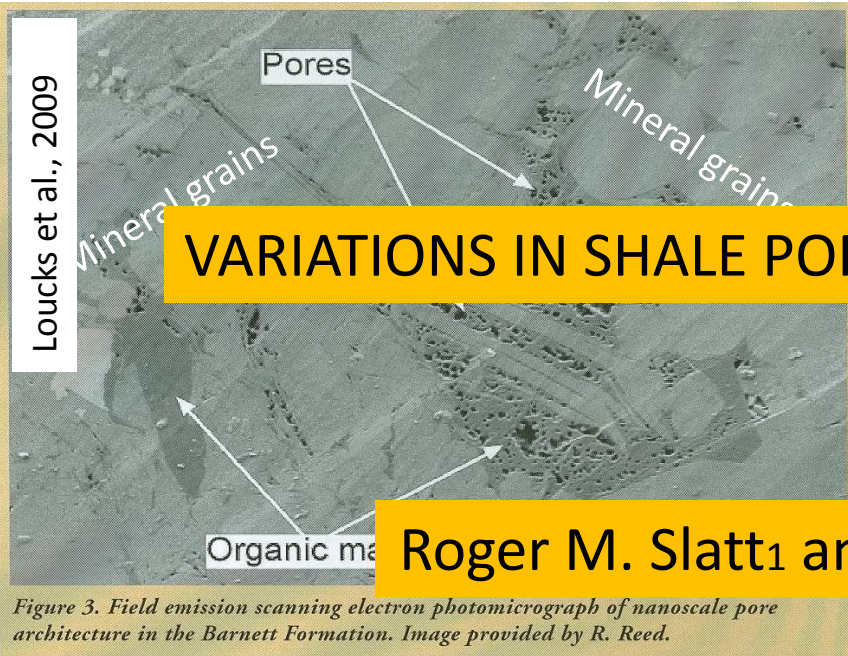
Slatt, R.M., and N.R. O'Brien, 2011, Pore types in the Barnett and Woodford gas shales: Contribution to understanding gas storage and migration pathways in fine-grained rocks, AAPG Bulletin, v.95, p. 2017-2030.

Sondergeld, C. H., R. J. Ambrose, C. S. Rai, and J. Moncrieff, 2010, Microstructural studies of gas shale: Society of Petroleum Engineers Unconventional Gas Conference, Pittsburgh, Pennsylvania, February 23–25, 2010, SPE Paper 131771, 17 p.

Wang, F.P., and R.M. Reed, 2009, Pore Networks and Fluid Flow in Gas Shales: SPE Annual Technical Conference and Exhibition, 4-7

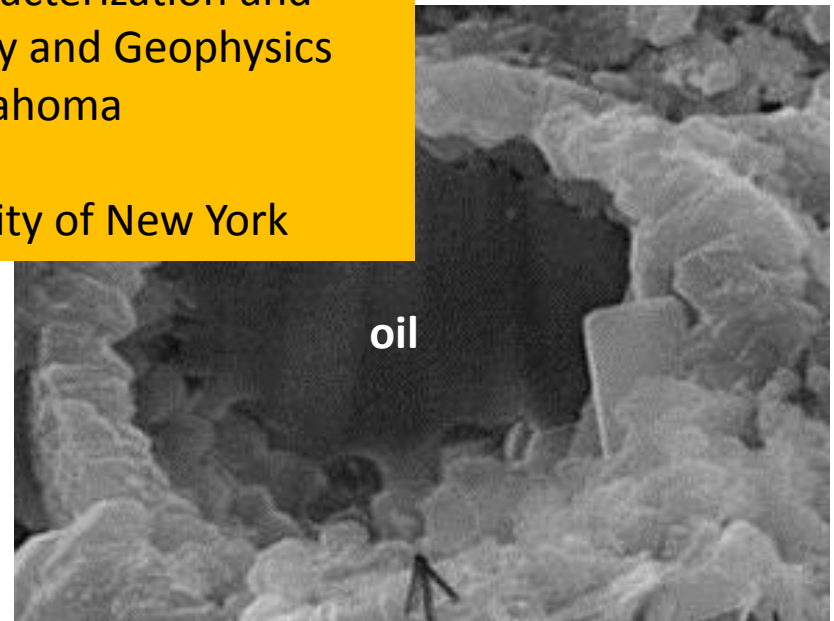
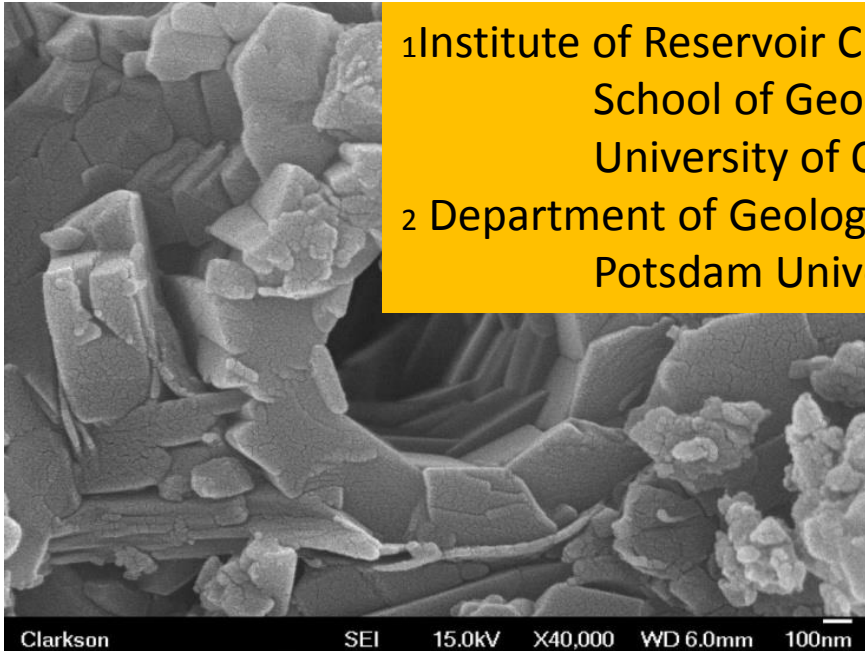
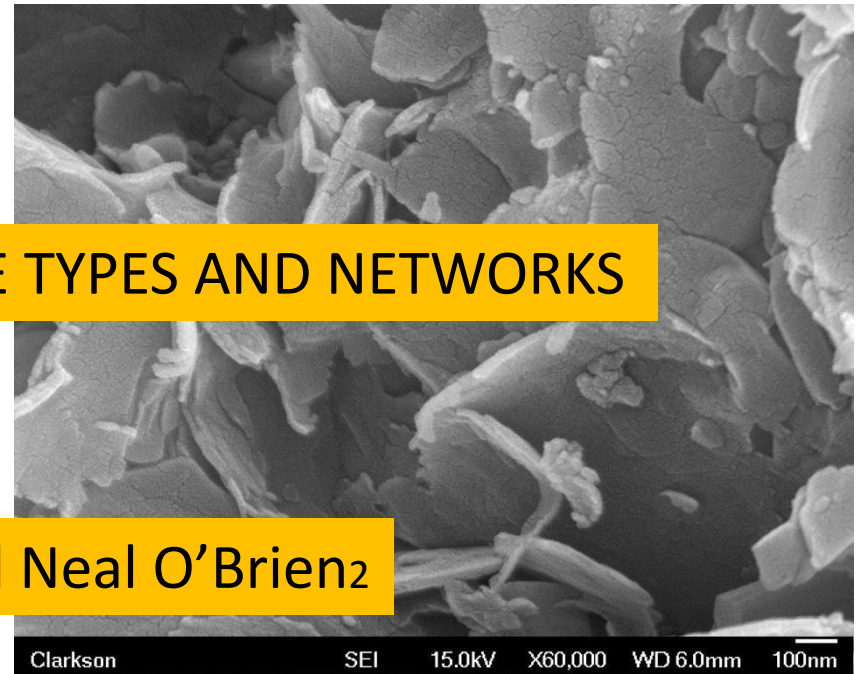
October 2009, New Orleans, Louisiana: SPE Document ID 124253-MS, 8 p.

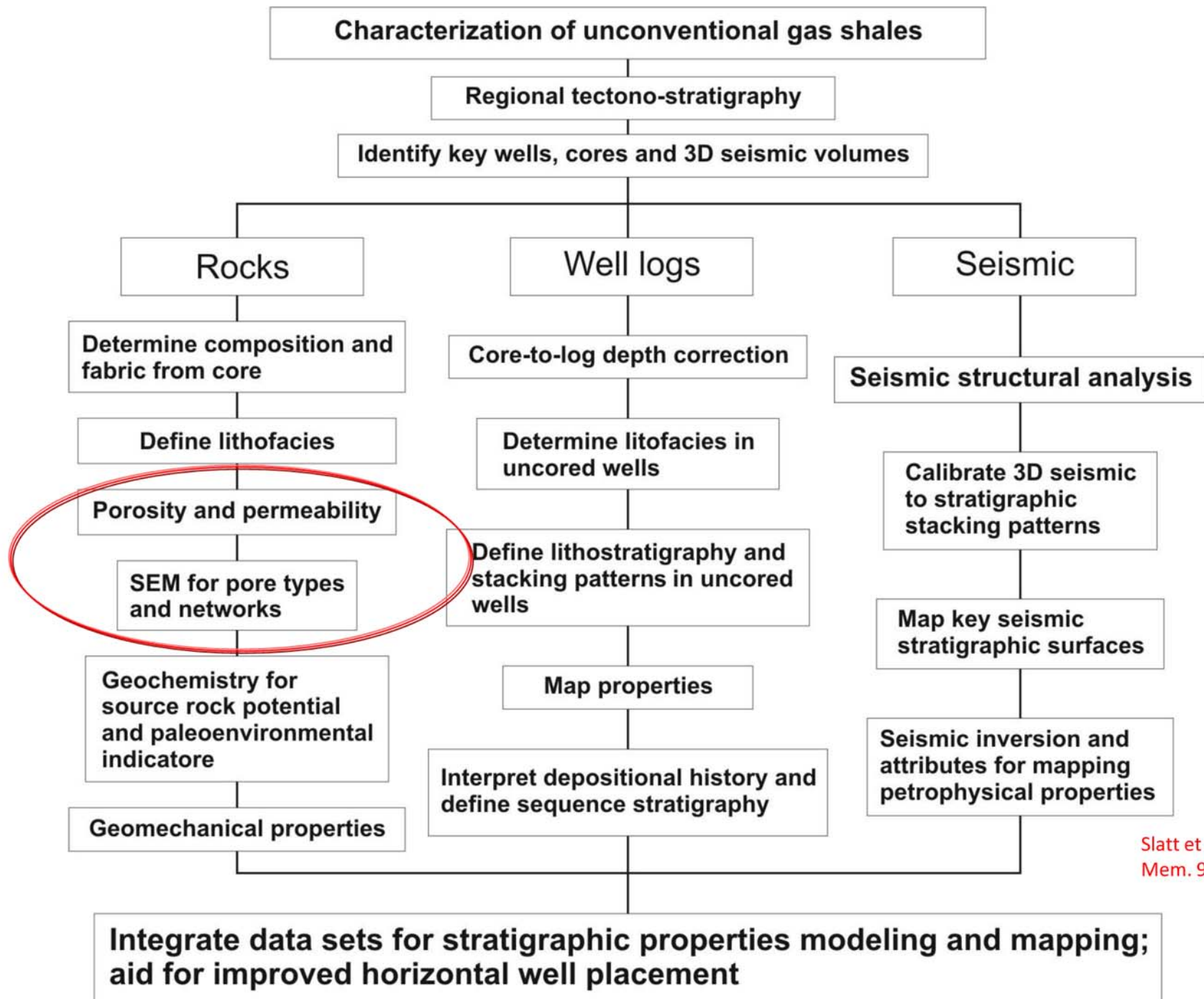
Wüst, R.A.J., B.R. Nassichuk, and R.M. Bustin, 2013, Porosity Characterization of Various Organic-rich Shales from the Western Canadian Sedimentary Basin, Alberta and British Columbia, Canada, *in* W.K. Camp, E. Diaz, and B. Wawak, eds., Electron Microscopy of Shale Hydrocarbon Reservoirs: AAPG Memoir 102, p.81-100.



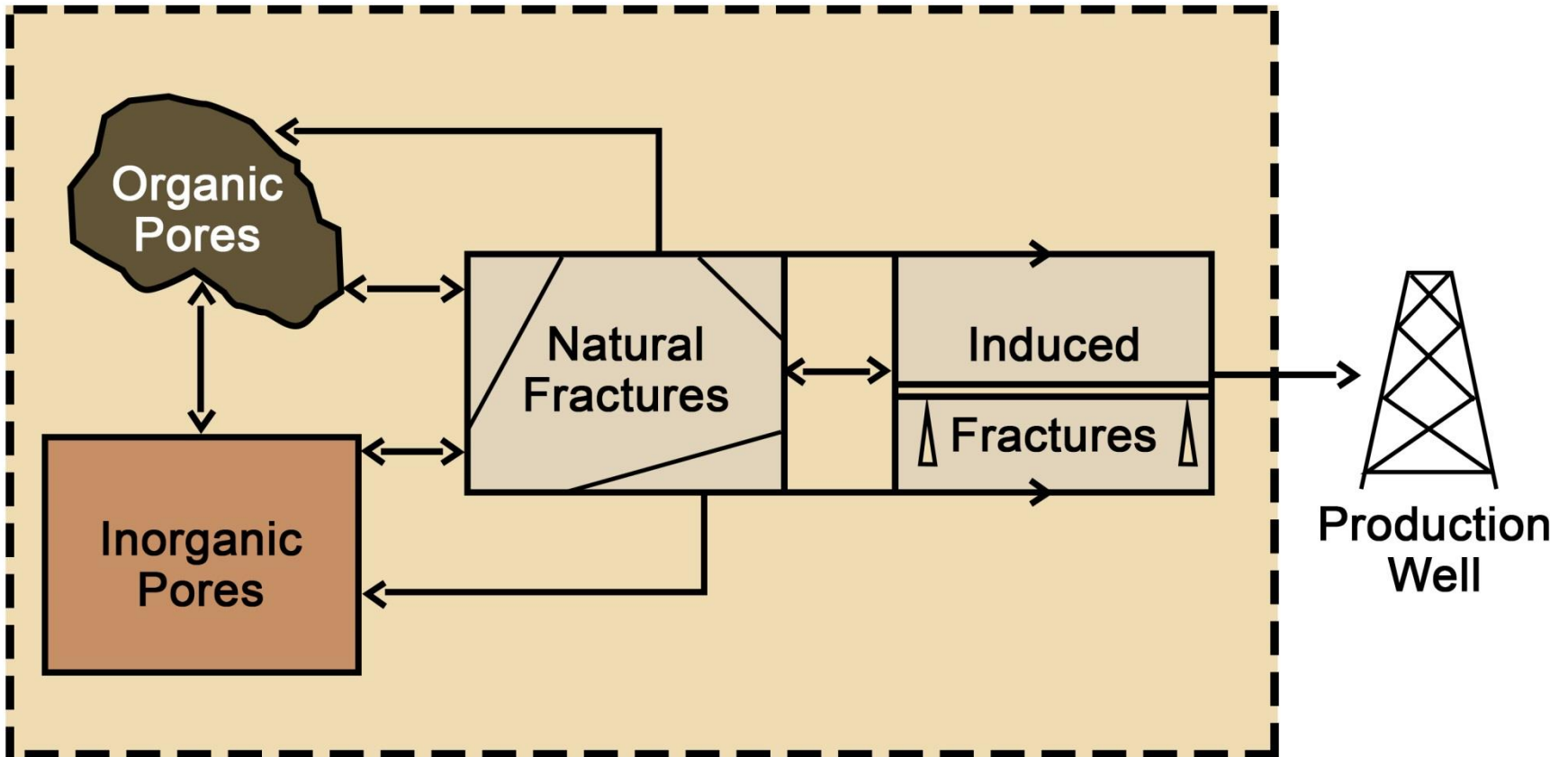
Roger M. Slatt¹ and Neal O'Brien²

¹Institute of Reservoir Characterization and
School of Geology and Geophysics
University of Oklahoma
² Department of Geology
Potsdam University of New York





Pores in Shales



Shale Gas Opportunities and Challenges*

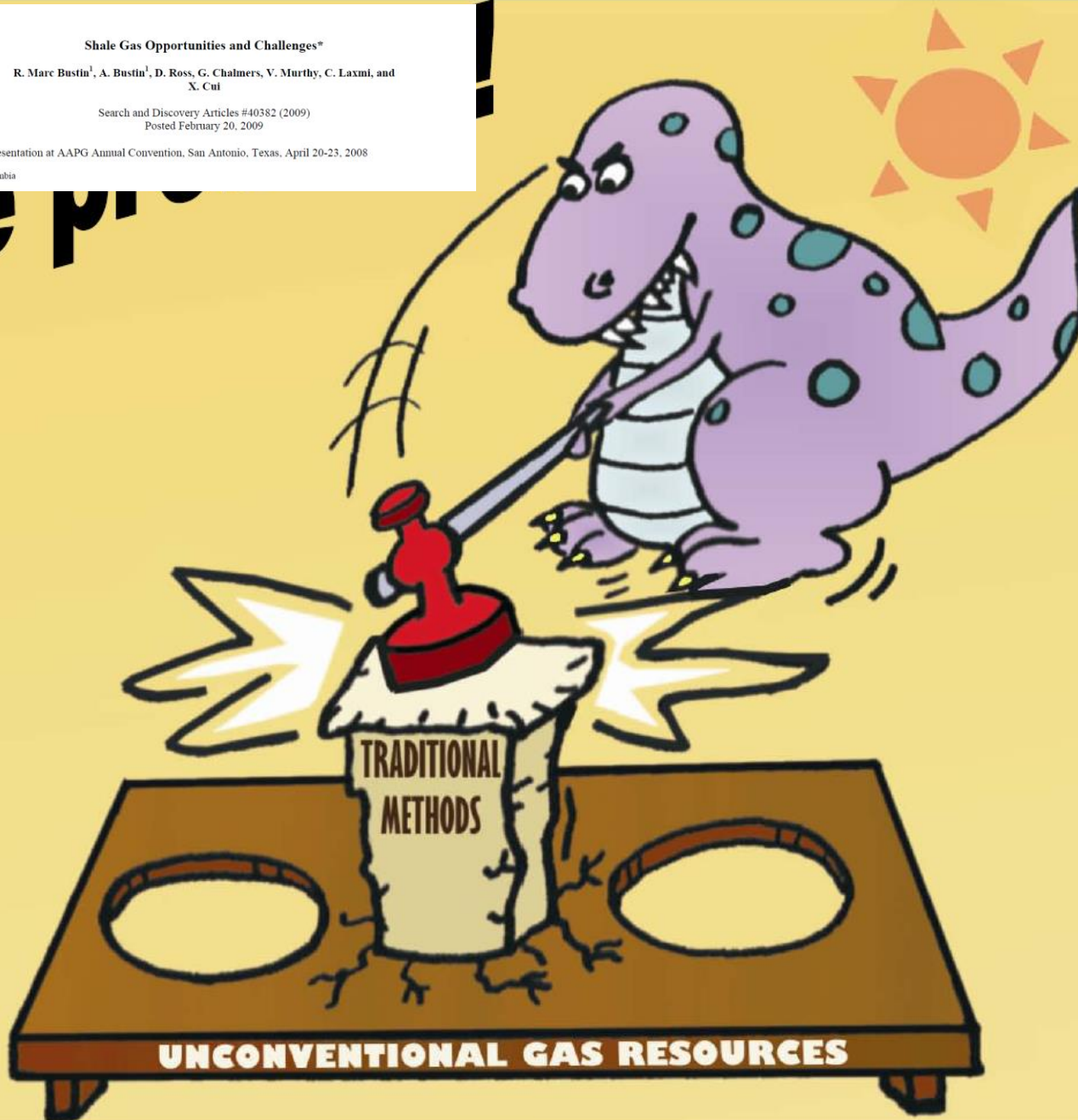
R. Marc Bustin¹, A. Bustin¹, D. Ross, G. Chalmers, V. Murthy, C. Laxmi, and X. Cui

Search and Discovery Articles #40382 (2009)
Posted February 20, 2009

*Adapted from oral presentation at AAPG Annual Convention, San Antonio, Texas, April 20-23, 2008

¹University of British Columbia

the p



Loucks, 2010

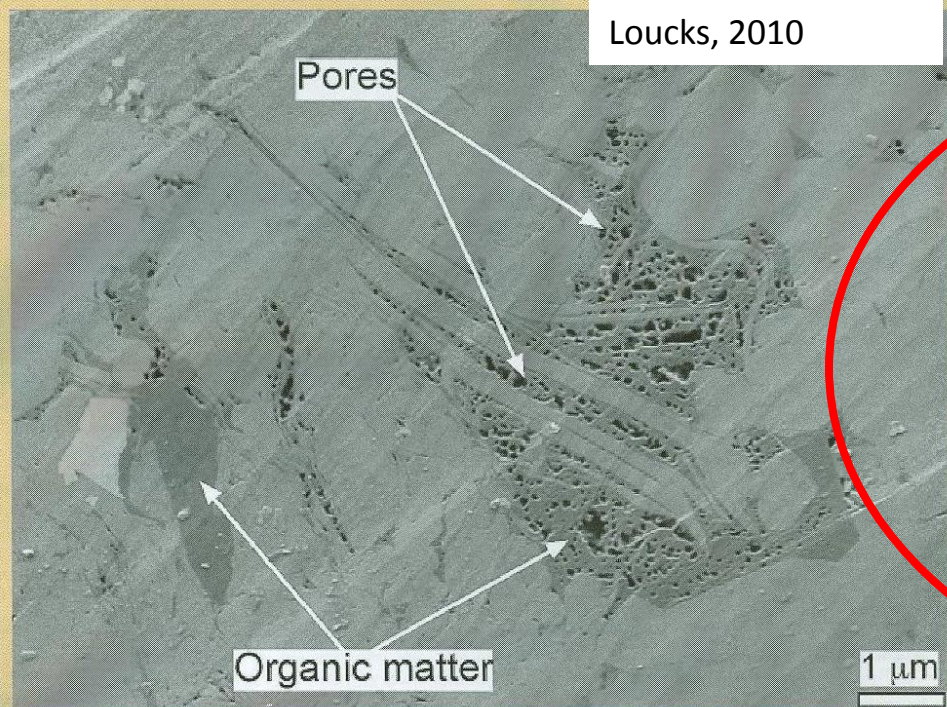
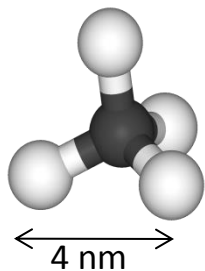
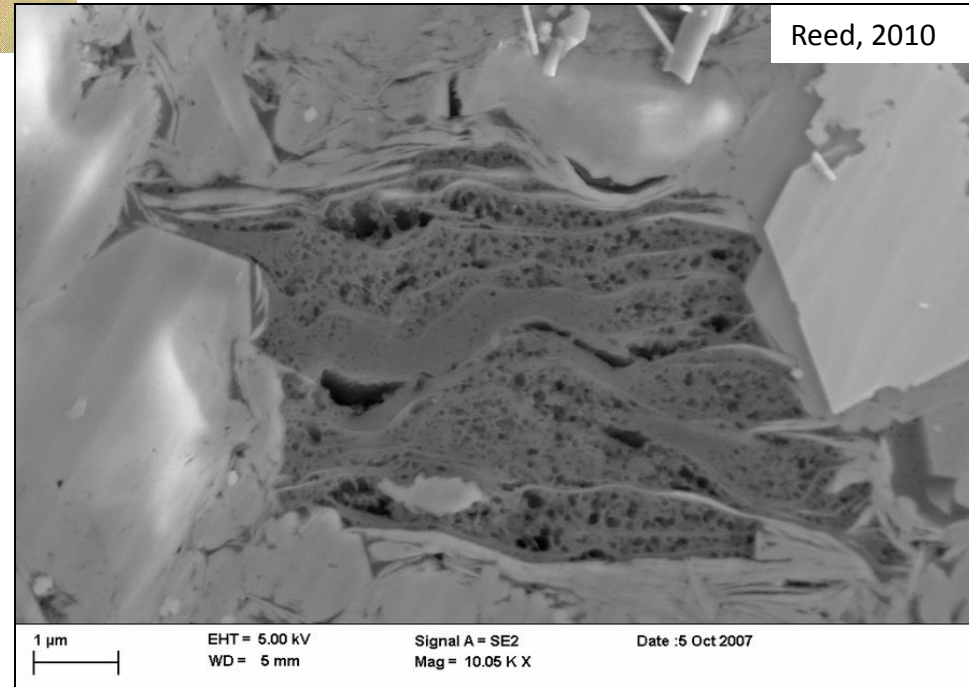


Figure 3. Field emission scanning electron photomicrograph of nanoscale pore architecture in the Barnett Formation. Image provided by R. Reed.

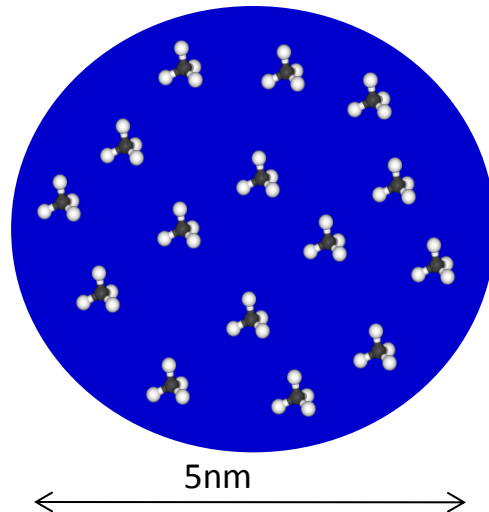
- Open porosity for “free” gas storage in “gas shales” is limited to nanopores in organics (kerogen).
- The observation is made that the rock matrix is (virtually?) devoid of porosity.
- Pores are formed as kerogen is converted to hydrocarbons resulting in the formation of liquids and gases.

Jarvie, et al., 2007

Reed, 2010

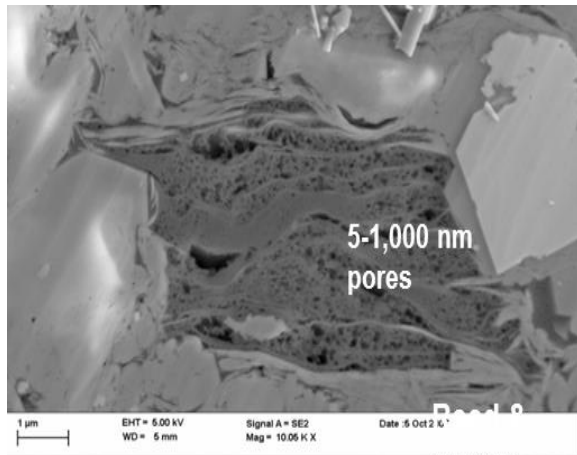


Loucks, 2010



Jarvie, D. M., 2012, *Shale resource systems for oil and gas: Part 2—Shale-oil resource systems*, in J. A. Breyer, ed., *Shale reservoirs—Giant resources for the 21st century: AAPG Memoir 97*, p. 89–119.

“With recent work in shale-gas resource systems, **it is evident that a part of the petroleum is trapped in isolated pore spaces associated with organic matter** (Reed and Loucks, 2007; Loucks et al., 2009) that were described as microreservoirs by Barker (1974). **These isolated pores contain free oil or gas** that rupture at the higher temperatures experienced during pyrolysis, thereby eluting in the Rock-Eval measured kerogen (S2) peak as do high-molecular-weight constituents of bitumen and crude oil.”



Reed and others, 2008

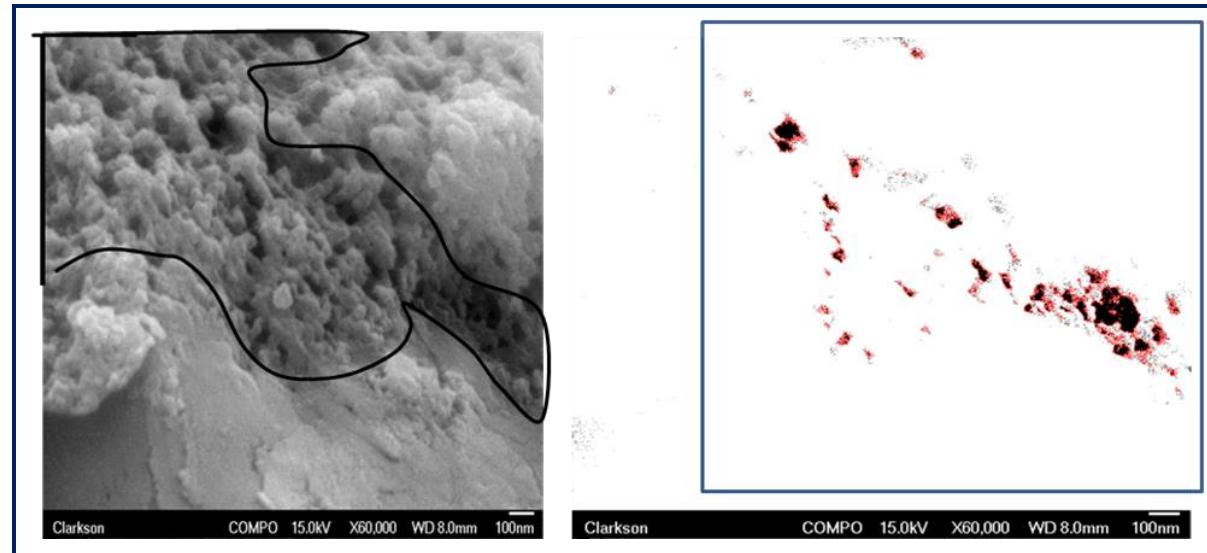
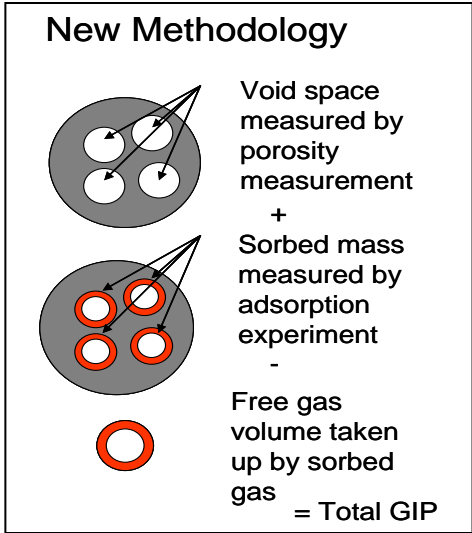


Figure 2. Kerogen sample with measured porosity. Porosity in outlined kerogen = 10.4%. Number of pores in outlined image = 244. Average pore area = $1.264 \mu\text{m}^2$. SEM image is of a freshly broken, untreated shale surface highlighting porous organic matter.

Ambrose, et al., 2010, New Pore-Scale considerations for shale gas in place calculations, SPE 13177

“Using FIB/SEM imaging technology, a series of 2D and 3D submicro-scale investigations are performed on the types of porous consitutents inherent to gas shale. **A finely dispersed porous organic (kerogen) material is observed imbedded within an inorganic matrix. The latter may contain larger-size pores of varying’geometries although it is the organic material that makes up the majority of gas pore volume, with pores and capillaries having characteristic lengths typically less than 100 nanometers. A significant portion of total gas-in-place appears to be associated with interconnected large nano-pores within the organic material.**” “.....the current industry standard disregards the volume (or organic pores) consumed by the sorbed phase, thus inadvertently overestimating the pore-volume available for free-gas storage.**In conclusion, a robust method that matches the local physics is presented to determine an accurate estimate of the gas-in-place in organic-rich gas shale.** “



AAPG Memoir 102: Electron Microscopy of shale hydrocarbon reservoirs

Editors: W. K. Camp, E. Diaz, and B. Wawak

Rine, J.M., E. Smart, W. Dorsey, K Hooghan, and M. Dixon.

“Analyzed samples from the Eagle Ford Group, Haynesville, Marcellus, and Barnett shales” “Within the sample set studied, **only the Barnett samples contained pores almost exclusively within organic particles.** For the characterization of nanometer-scale pores, SEM examination of Ar-Ion milled samples was a far superior methodology to thin-section petrography and standard (broken sample) SEM examinations”

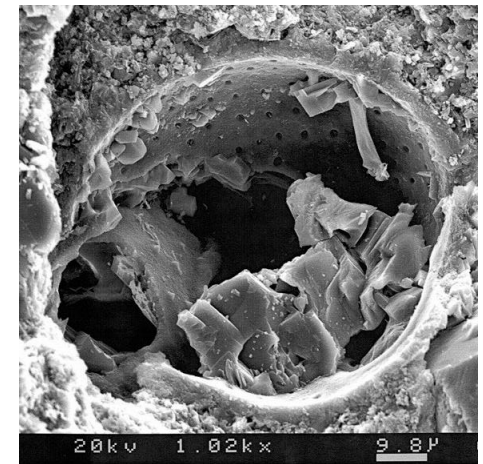
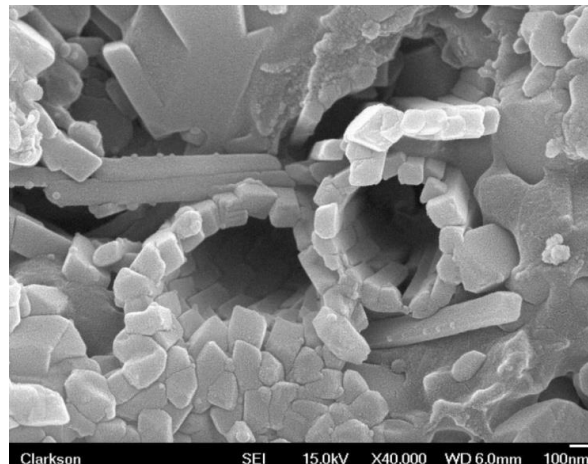
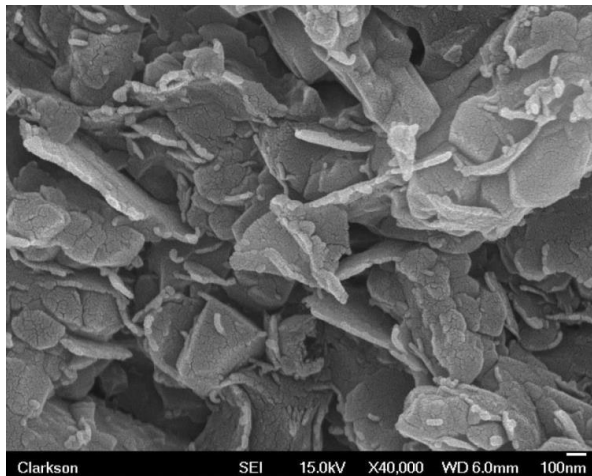
Erdman and Drenzek: “**The siliceous Barnett, for example, displays abundant organic-matter-hosted pores with less mineral porosity,** similar to previous observations (Loucks et al., 2009; Wang and Reed, 2009; Loucks et al., 2010; Milner et al., 2010; Sondergeld et al., 2010), whereas micrometer- to nanometer-size pores in the argillaceous **Marcellus sample appear to be predominantly associated with organic-clay mineral interfaces** as likewise reported by previous studies (Milner et al., 2010; Curtis et al., 2011). These mixed-porosity systems are bracketed by the behavior of the calcareous **Haynesville**, for which the high level of thermal Maturity ($T_{max} = 512^{\circ}\text{C}$, $V_{re}=2.4\%$) has led to a **greater abundance of larger organic matter-hosted pores**; and of the Carbonaceous **Woodford shale**, in which a **pore network has yet to clearly develop** in its abundant, yet thermally immature ($T_{max} = 435^{\circ}\text{C}$, $V_{re}=0.6\%$) organic matter inventory. **Indeed, mineral based pores** (perhaps volumetrically dominated by diagenetic pyrite) **may represent the only viable storage and migration pathways for oil and wet gas production from relatively low-maturity shale plays.....”**

AAPG Memoir 102: Electron Microscopy of shale hydrocarbon reservoirs

Editors: W. K. Camp, E. Diaz, and B. Wawak


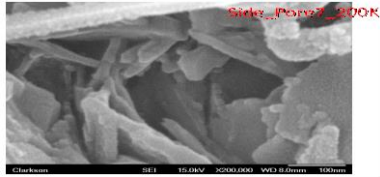

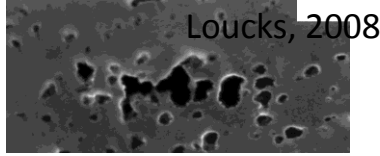

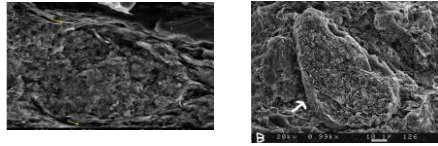
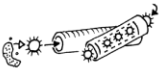
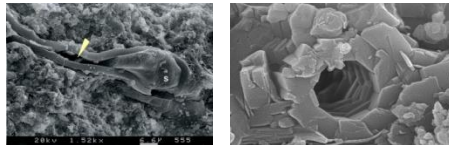

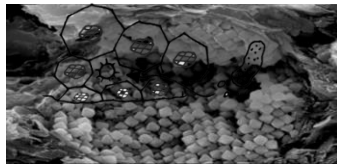
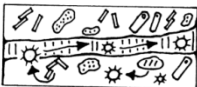
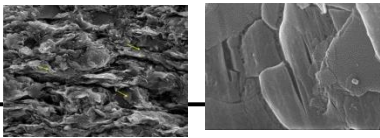
Jennings and Antia: Petrographic characterization of the Eagle Ford Shale, south Texas: Mineralogy, common constituents and distribution of nanometer-scale pore types.

"The most abundant pore types in southwestern Gulf Coast Basin samples were interparticle (between coccolith fragments and plates) and intraparticle pores (within coccoliths, locally Common fecal pellets, foram chambers, recrystallized foraminifera, plagioclase grains, and pyrite framboids.....SEM data revealed that Eagle Ford shales in the southwestern Gulf Coast Basin displayed higher porosity and higher permeability than samples from the Eagle Ford and Maness shales in the eastern Texas basin, which is likely because of the presence of well-connected interparticle and intraparticle pores between abundant coccolith fragments.....Although organic nanopores were typically most abundant in organic-rich marls with abundant coccolith fragments and fecal pellets, vertical variability in the presence and abundance of organic nanopores in all microfabrics was common."

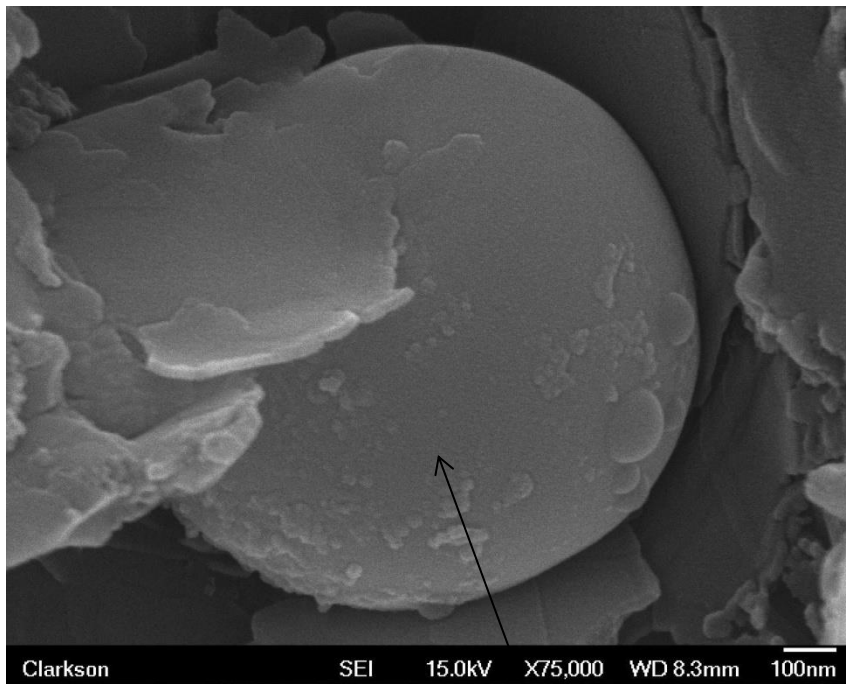


SEM images of Eagle Ford provided by O'Brien

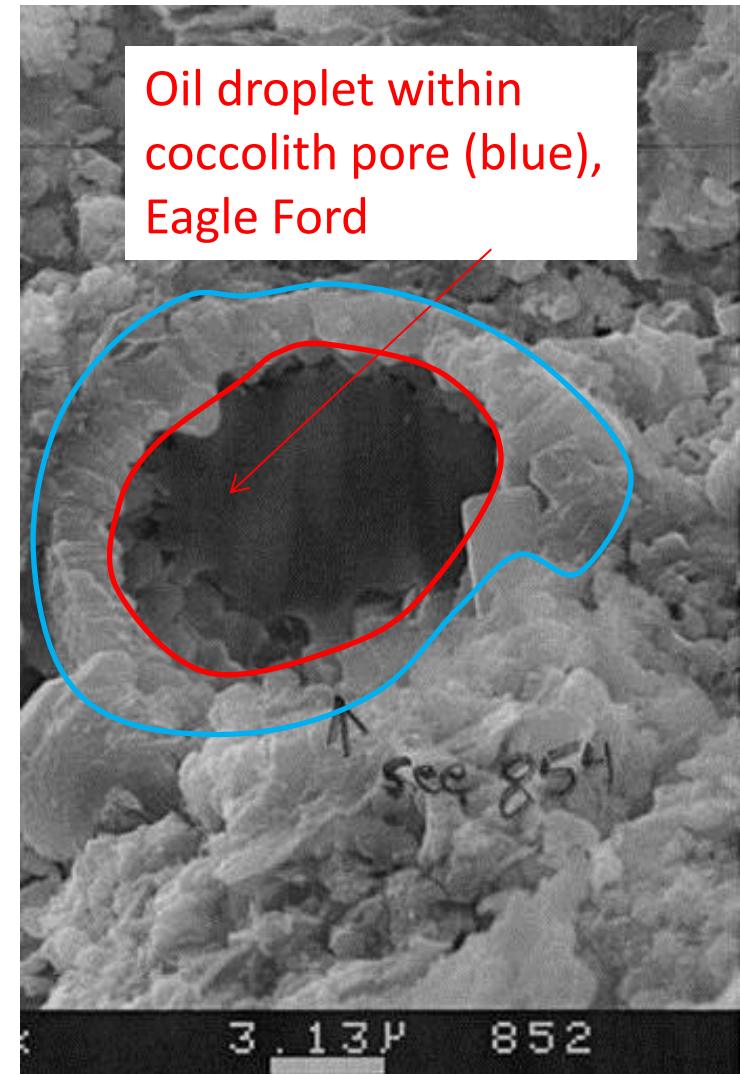
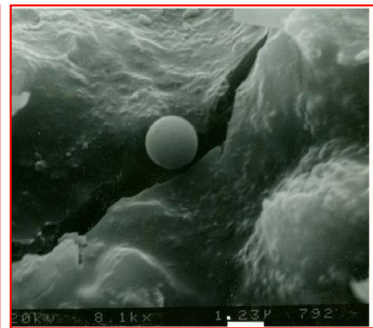
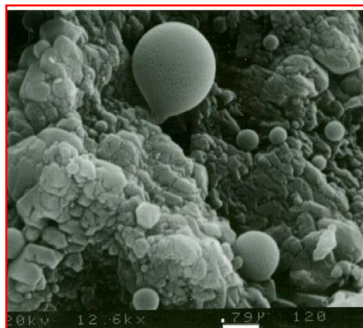
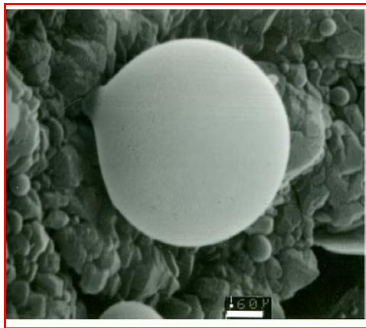
Multiple pore types

Pore Type	Image	Distinctive Features
Porous Floccules 		Clumps of electrostatically charged clay flakes arranged in edge-face or edge-edge cardhouse structure . Pores up to 10's of microns in diameter. Pores may be connected.
Organo-porosity 		Pores in smooth surfaces of organic flakes or kerogen . Pore diameters are at nanometer scale . Pores are generally isolated. Porous organic coatings can also be adsorbed on clays.
Fecal Pellets 		Spheres/ellipsoids with randomly oriented internal particles, giving rise to intrapellet pores . Pellets are sand-size and may be aligned into laminae.
Fossil Fragments 		Porous fossil particles , including sponge spicules, coccoliths, radiolaria, and cysts (<i>Tasmanites</i> ?). Interior chamber may be open or filled with detrital or authigenic minerals.
Intraparticle Grains/Pores 		Porous grains , such as pyrite framboids which have internal pores between micro-crystals. Grains are of secondary origin, and are usually dispersed within the shale matrix.
Microchannels and Microfractures 		Linear nano-micrometer-sized openings that often cross-cuts bedding planes. Occur at nano-meter and larger scales.

Slatt and O'Brien, 2011, Pore types in the Barnett and Woodford gas shales: contribution to understanding gas storage and migration pathways in fine-grained rocks, AAPG Bull, Dec



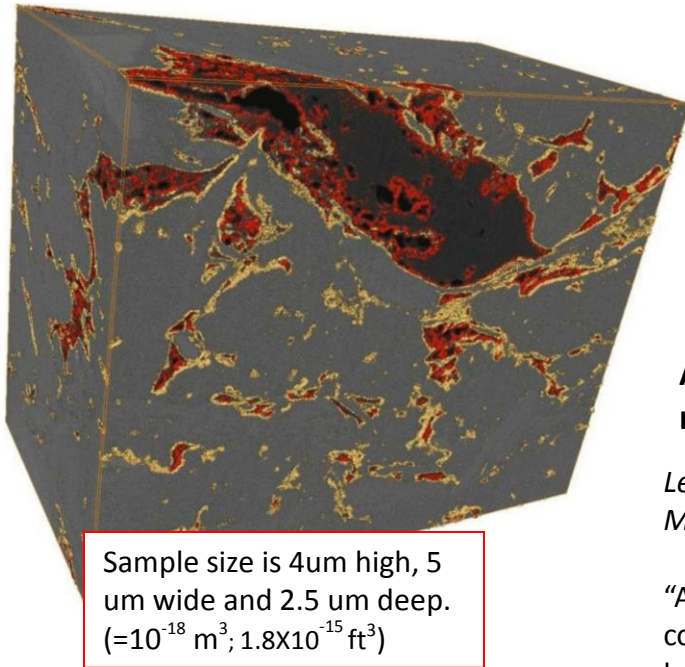
Unheated (natural) Horn River oil droplet



Oil droplet within
coccolith pore (blue),
Eagle Ford

SEM micrographs of the Woodford and Eagle Ford shales during hydrous pyrolysis experiment – heating to 350°C for 4 days.

Ar (or Ga)-Ion-Beam Milling



Ambrose et al., 2010. "Fig. 5. 3-D FIB/SEM segmentation showing porosity and kerogen network, yellow outlines the 3-D kerogen network., red outlines porosity (in this sample all porosity is found within the kerogen)".

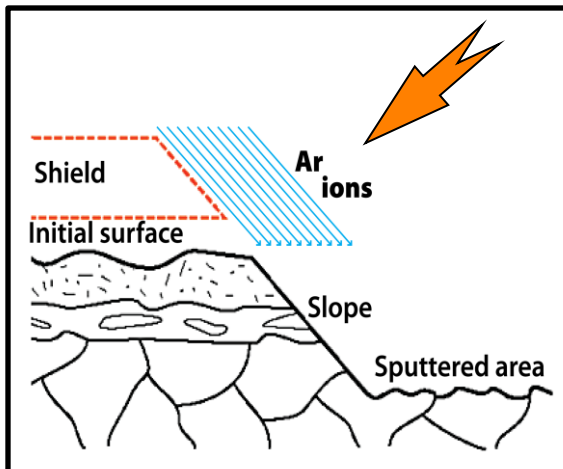
AAPG Memoir 102: Electron Microscopy of shale hydrocarbon reservoirs Editors: W. K. Camp, E. Diaz, and B. Wawak

Lemmens and Richards,
Multiscale imaging of shale samples in the Scanning Electron Microscope;

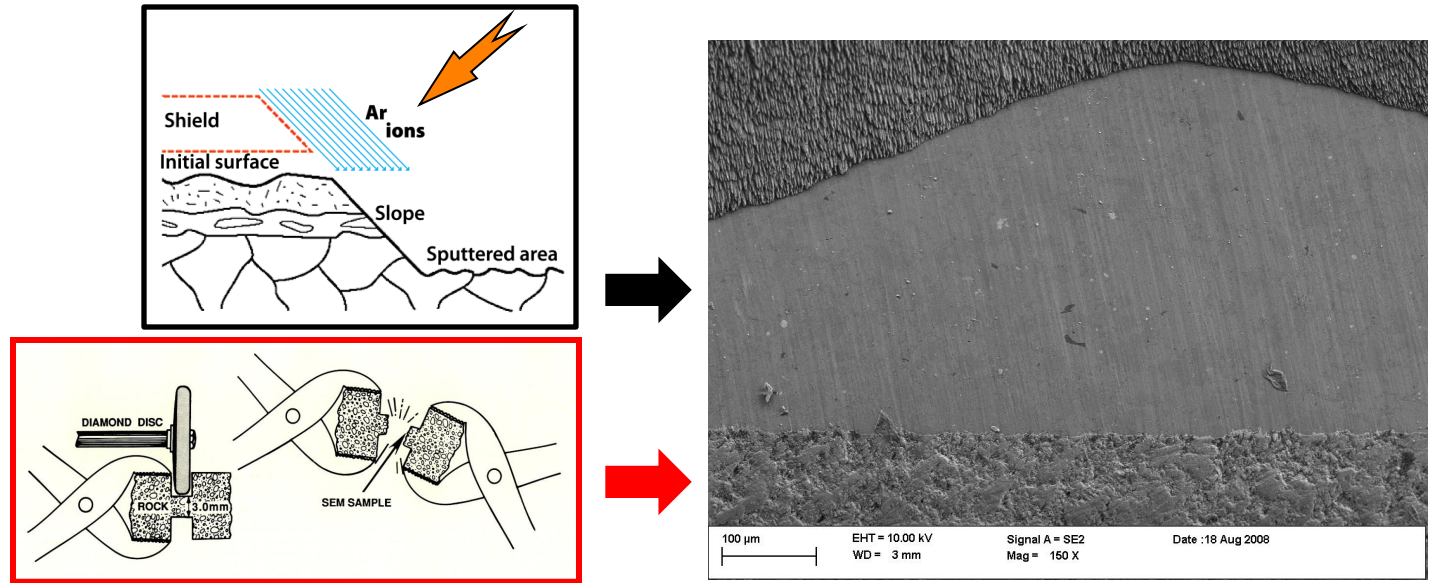
"A typical FIB-SEM takes this even one step further by providing a 3D data set composed of hundreds of such high-resolution SEM images. A typical FIB-SEM data set has a spatial resolution of 10nm for a volume of 10X10X10um."

"A most relevant question is how representative those small-volume FIB-SEM data sets are.For a 1 inch core plug, this still means that <1% of the sample surface is actually imaged at a resolutionable to resolve the porosity before deciding where to perform an FIB-SEM experiment."

"The risk associated with the much higher resolution characterization of shale core sample material with high resolution SEM and FIB-SEM is that the structural association with fabric is lost. Yet fabric heterogeneity is equally important for the characterization of shale samples, and the association of nanometer scale pore structures with fabric domains may provide important information on permeability and fluid flow at the scale of the core. Tiling and stitching SEM images into mosaics enable pore-scale resolution over the entire core plug surface in one image."



SEM SAMPLE PREPARATION



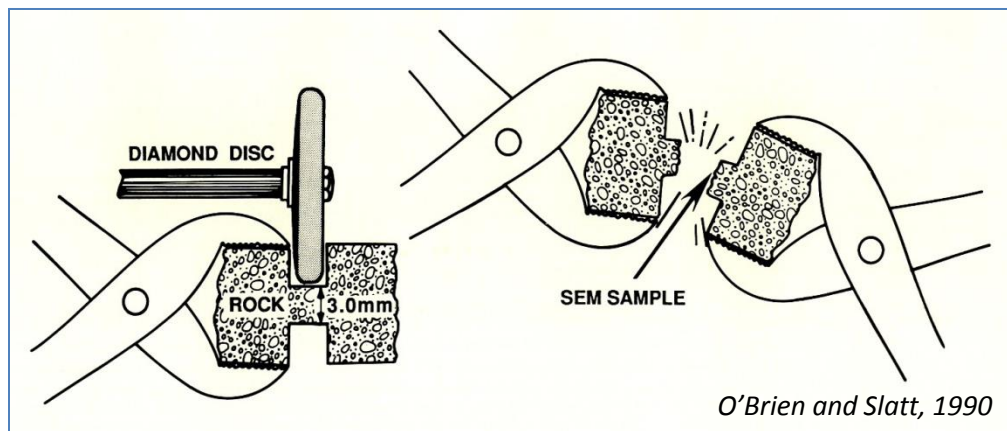
O'Brien and Slatt, 1990

AAPG Memoir 102: Electron Microscopy of shale hydrocarbon reservoirs

Editors: W. K. Camp, E. Diaz, and B. Wawak

Lemmens and Richards: “The risk associated with the much higher resolution characterization of shale core sample material with high resolution SEM and FIB-SEM is that the structural association with fabric is lost. Yet fabric heterogeneity is equally important for the characterization of shale samples, and the association of nanometer scale pore structures with fabric domains may provide important information on permeability and fluid flow at the scale of the core. Tiling and stitching SEM images into mosaics enable pore-scale resolution over the entire core plug surface in one image.”

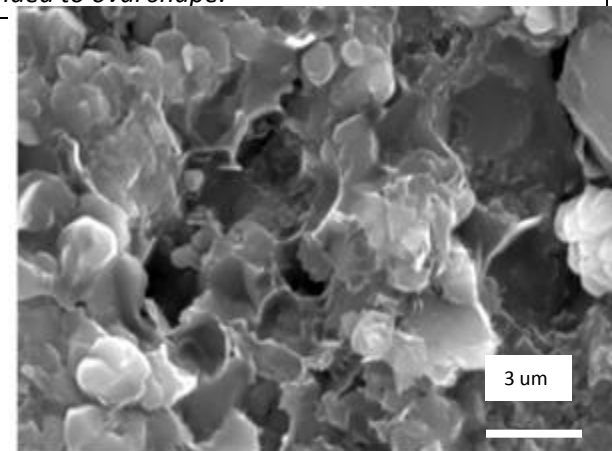
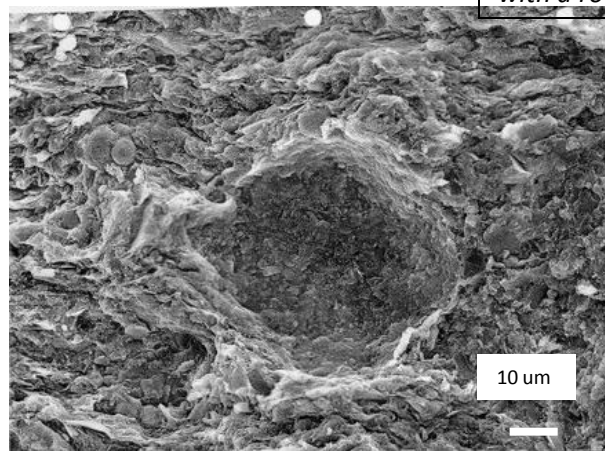
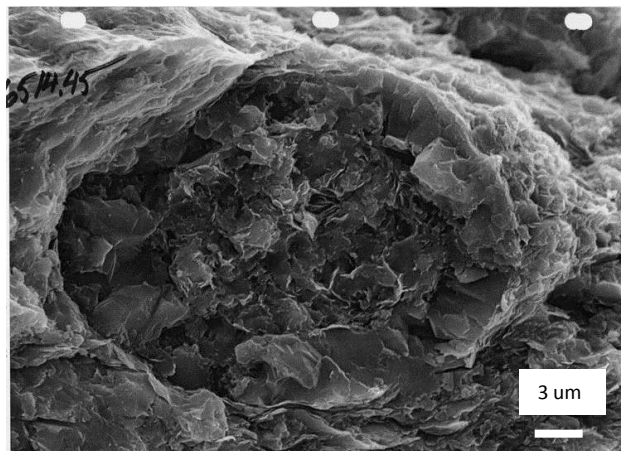
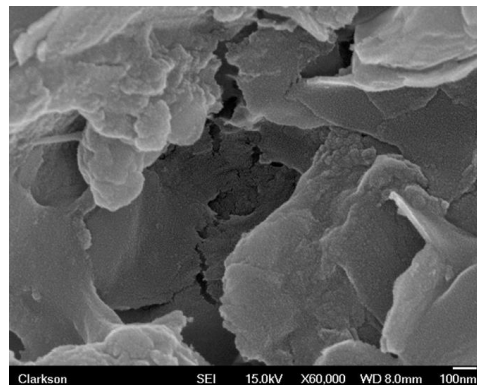
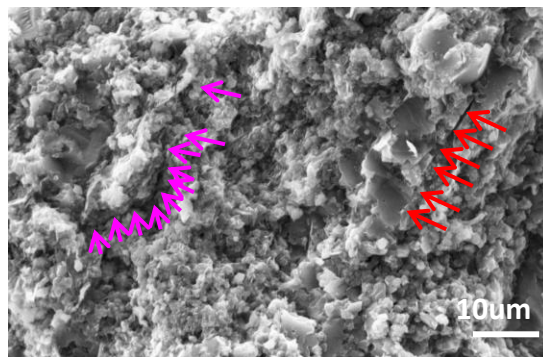
ConventionL SEM sample prep.: With a bit of experience you can identify plucked grain-holes



AAPG Memoir 102: Electron Microscopy of shale hydrocarbon reservoirs, Editors: W. K. Camp, E. Diaz, and B. Wawak:

Wust et al studied organic rich shales in Western Canada Sedimentary Basin: "It was suggested that the larger pores in conventional SEM analysis may be caused by grain plucking during sample preparation (Sondergeld et al., 2010). The morphological analyses of this study indicated, however, that grain plucking was relatively rare and could easily be identified and excluded in pore size measurements."

Our (Slatt, O'Brien and others) studies have shown that experience allows one to differentiate real pores from artifacts of sampling. The method we use is shown in the top figure (from O'Brien and Slatt, 1990). The middle left image shows an irregular-shaped tear produced during sample breaking (purple arrows) and a straight natural microfracture (red arrows). The middle center figure shows a tear in a shale sample. The lower images are of broken surfaces: left image is a fecal pellet...note the tangentially oriented clay flakes compacted around the pellet. The lower middle image clearly shows a plucked grain hole because the compacted tangential clay flakes retain the structure of the plucked grain. Lower right figure shows pop-out holes with a rounded to oval shape.



Low cost porosity determination from conventional SEM

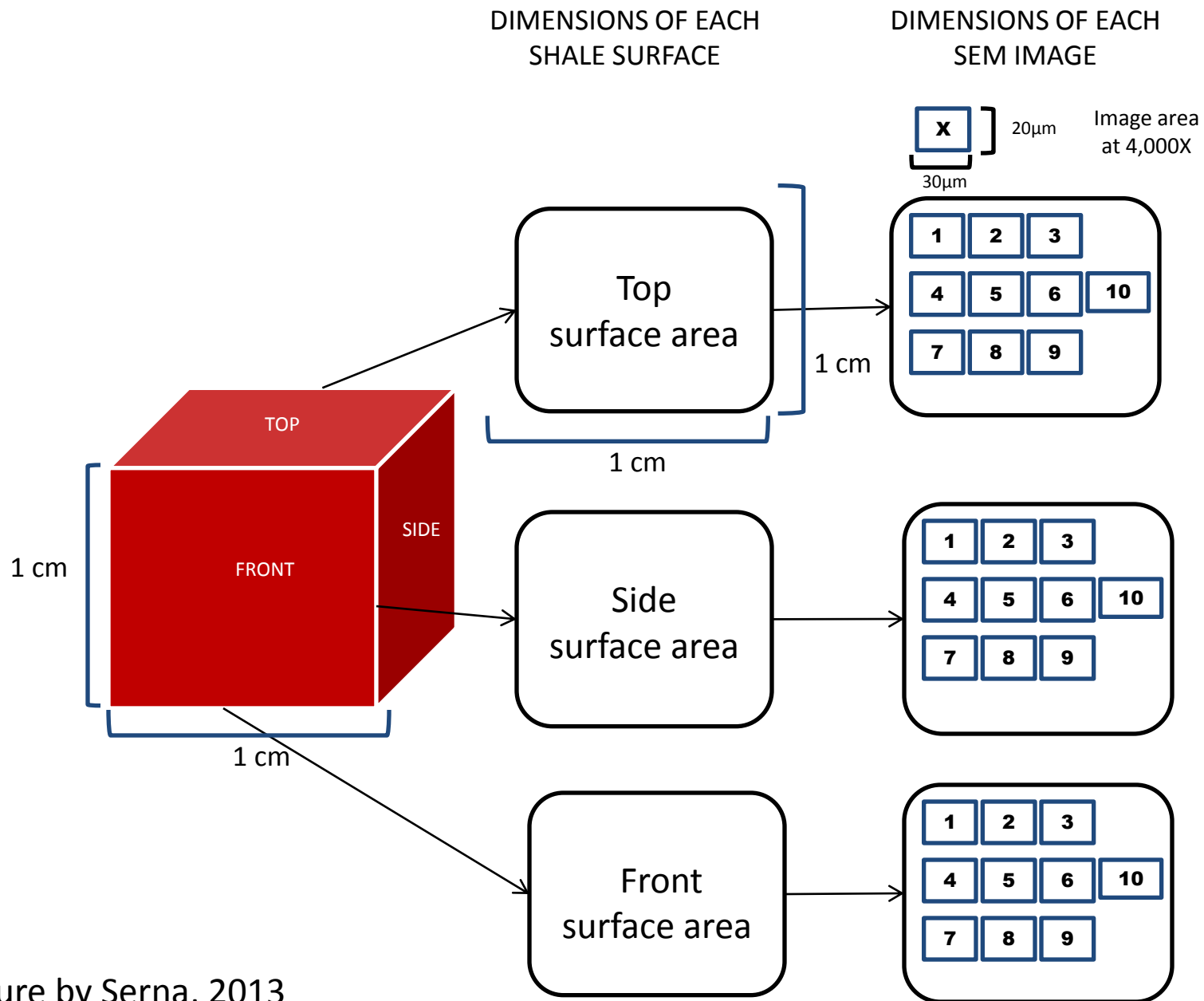
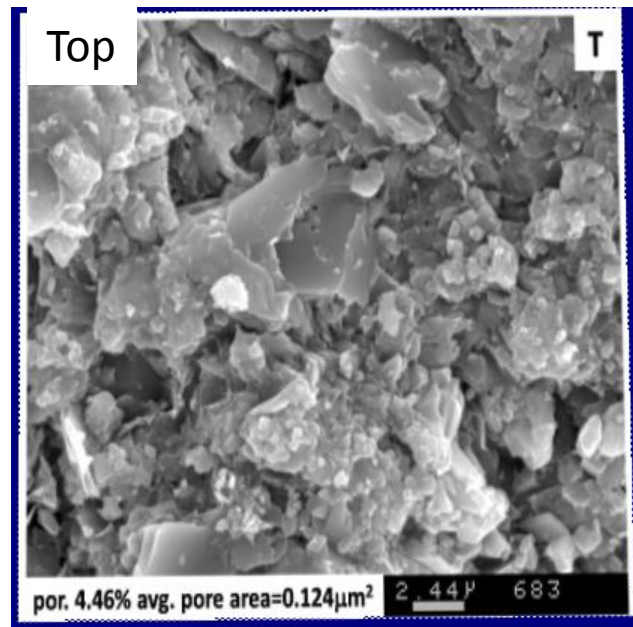
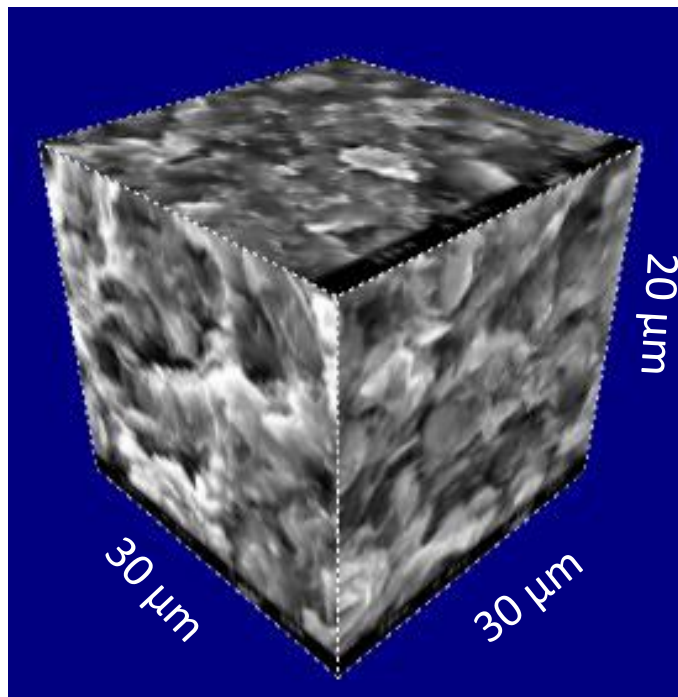
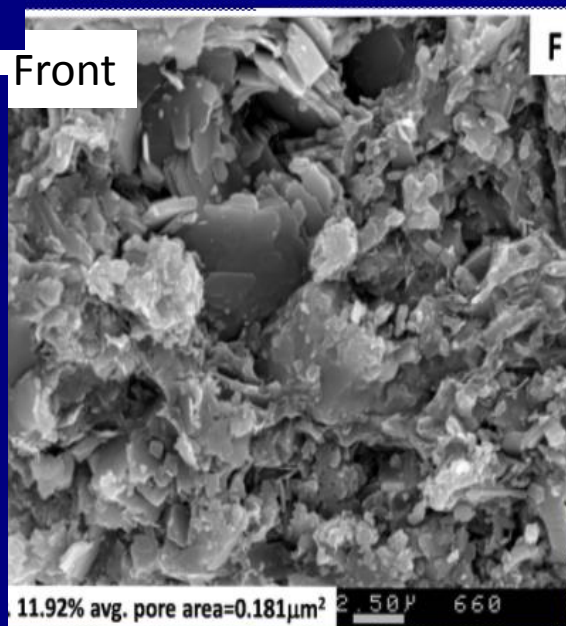
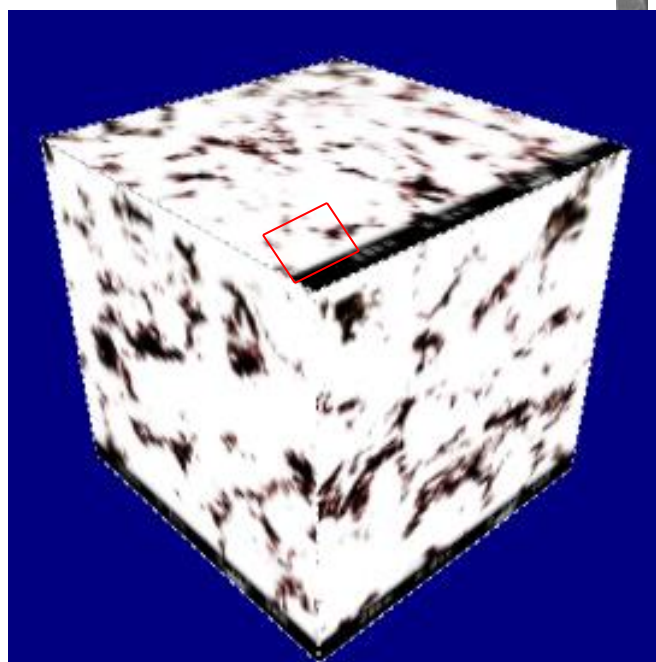


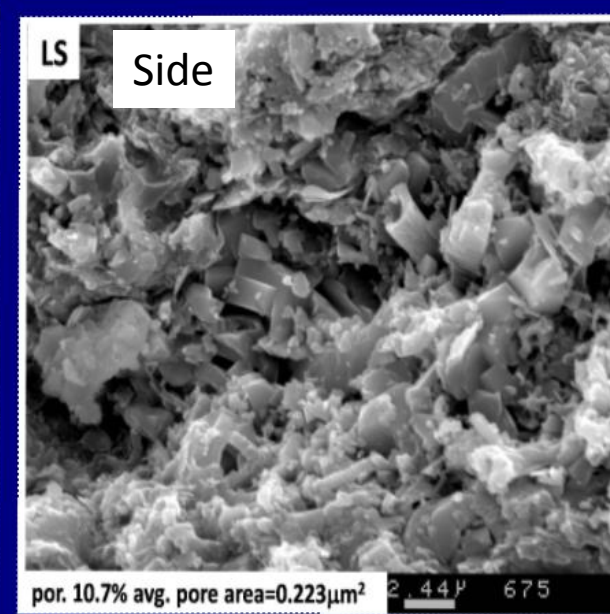
Figure by Serna, 2013



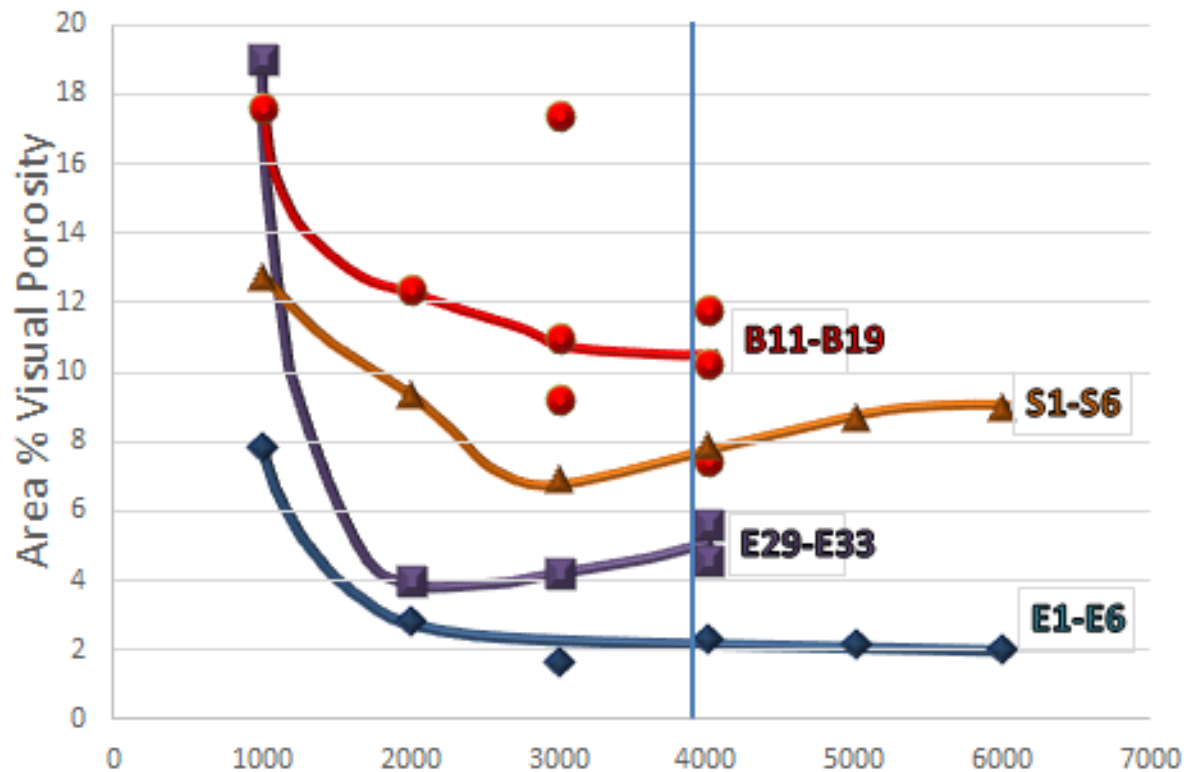
4.5% por.



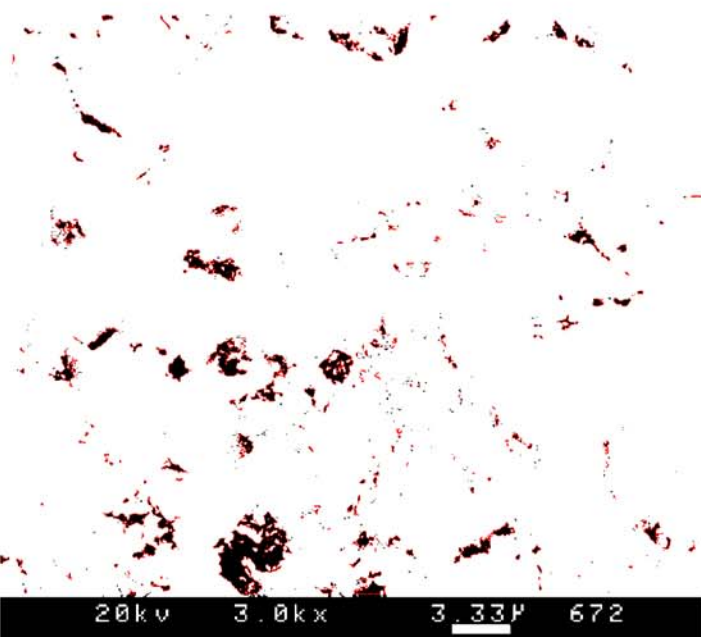
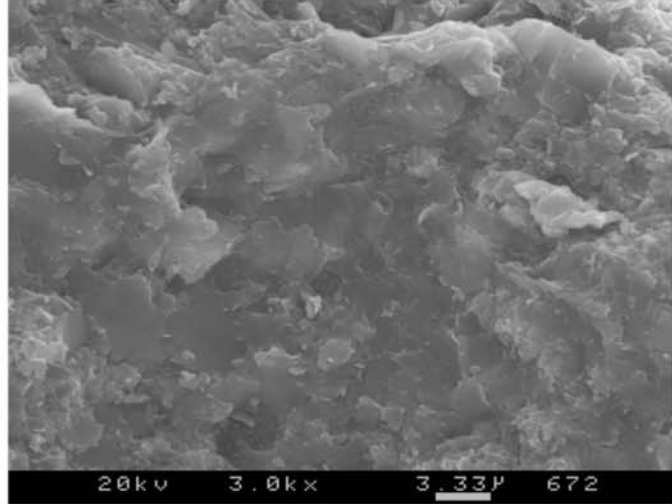
11.9% por.



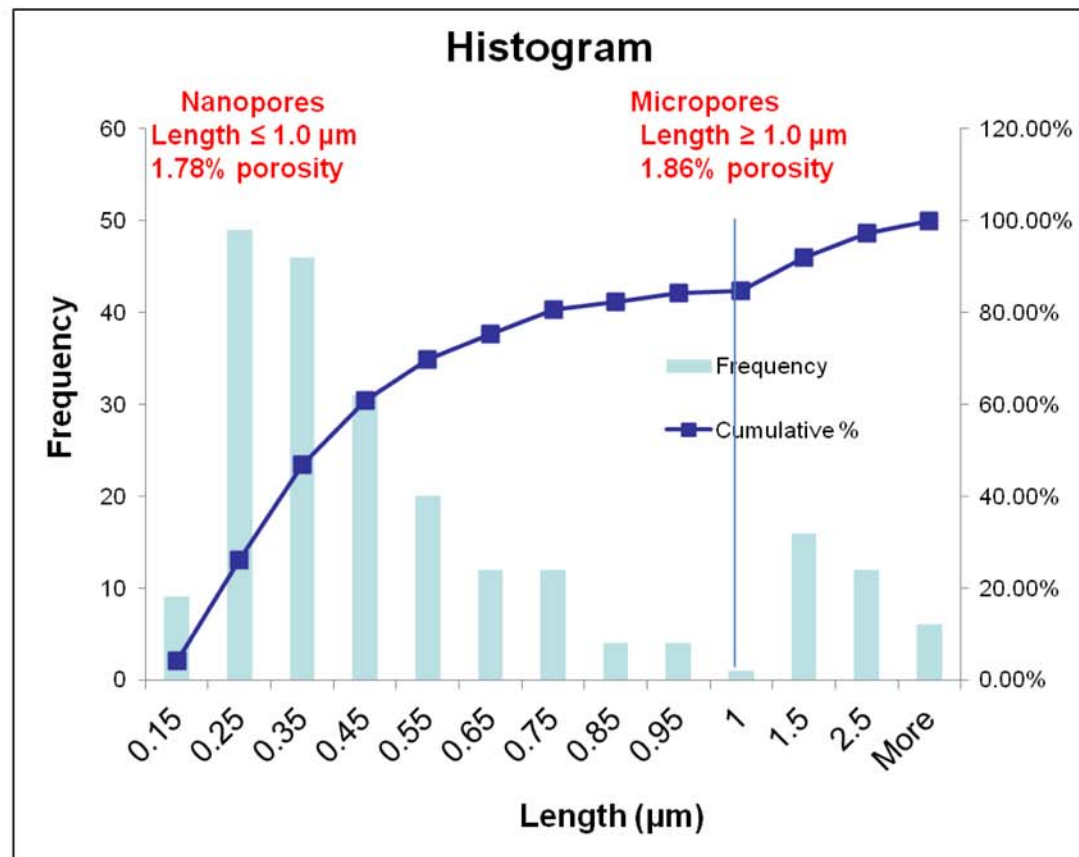
10.7% por.



SEM magnifications vs. area % visual porosity for four shale surfaces. In each case, above 2,000-3,000X magnification, the % porosity does not change significantly. A magnification of 4,000X (shown by the vertical blue line) was selected as the standard magnification for our pore studies.

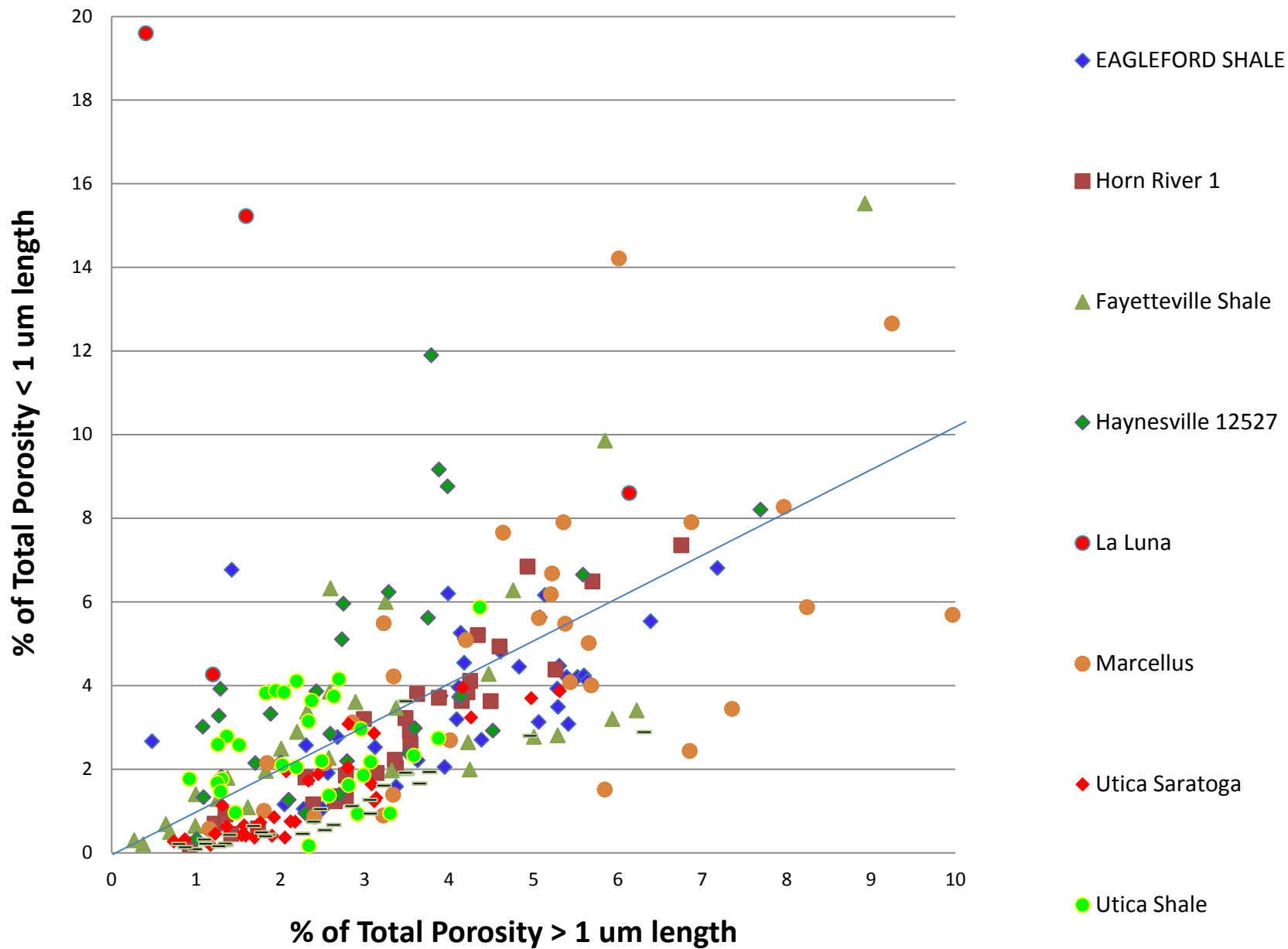


Porosity calculated: 3.64%
 Number of pores: 222
 Average area (μm^2): 0.168



Abundance of Nanopores vs. Micropores
 Based upon 2D long axis of pores

Shale	SHALE PORE DATA X porosity (area %)				Xpore area (μm ²)	Main inorganic pore types
	top	front	side	Aver.		
EagleFord (B1)	4.4	4.4	3.9	4.2	0.033	Flocs, Coccoliths, Microchannels
EagleFord1 6.4	9.5	7.7	8.1			
EagleFord2 6.2	9.8	6.8	7.4	0.192		
Fayetteville 2.3	10.3	6.5	6.4	0.195		Microchannels, pellets
Haynesville07	6.7	16.0	17.8	13.5	0.211	Pellets, coccoliths, microchannels
Haynesville27	5.0	8.4	7.7	7.0	0.171	
Horn River1 3.3	8.3	6.4	6.0	0.117		Flocs (cemented)
Horn River2 7.0	9.3	10.3	8.9	0.121		
LaLuna				14.7	0.329	Microchannels,flocs
Marcellus (1-3)	4.5	6.6	6.3	5.8	0.046	Flocs, microchannels, microfractures
Marcellus AK70	9.0	10.4	9.9	9.8	0.145	
Woodford 4.8	8.4	6.4	6.5			Pellets, Tasmanites, Flocs
(All measurements at X4000 except Woodford at X8000 magnification)						



Institute of Reservoir Characterization



PATHFINDER EXPLORATION, LLC

